PHYSICAL REVIEW VOLUME 66, NUMBERS 7 AND 8 OCTOBER 1 AND 15, 1944

The Paths of Ions and Electrons in Non-Uniform Magnetic Fields*

NORMAN D. COGGESHALL AND MORRIS MUSKAT
Gulf Research and Development Company, Pittsburgh, Pennsylvania
(Received July 29, 1944)

The integration of the Lorentz force equations to give electron or ion paths has been reduced to simple quadratures for systems in which the electric field is zero and the magnetic field is a function of one Cartesian or cylindrical coordinate. For several interesting types of magnetic field variation the quadrature can be carried through analytically; and even for complicated magnetic fields, or such as are known only empirically, the numerical integration can be effected without difficulty. From general considerations of the functions involved, it is possible to determine the extension and periodicity of the orbits for any set of initial conditions. The representation used is also convenient for obtaining information regarding the dispersion and focusing characteristics of the trajectories, some of which have unique properties of promise for use in specific instrument design such as mass spectrometers, beta-ray spectrographs, etc. Schematic designs of such instruments are proposed, and a discussion is given of their advantages and special properties.

INTRODUCTION

THE focusing and dispersing properties of a uniform magnetic field have been applied with great success in recent years to mass spectrographs, mass spectrometers, and β-ray spectrometers, as well as to more special uses.

Many instruments have been built and described which employ either 180° focusing or the focusing properties of sector-shaped magnetic fields. All are generically of the same class, of which the 360° analyzer is the only one having the property of perfect focusing. However, it is not practical to attempt to utilize the latter because of the physical impossibility of locating both a source of ions and a collector at exactly the same place.

In contrast to the wide application of the focusing and dispersing properties of a uniform magnetic field, little use has been made of the focusing properties of non-uniform fields. The problem of calculating paths, dispersion, and focusing characteristics for a general type of non-uniform field is one of great mathematical difficulty.[1] There are, however, some cases of considerable physical interest in which the magnetic field varies in a fairly simple manner, and for which it is possible to calculate exactly the paths, dispersion, and focusing properties.

In all cases where the pole faces of a magnet or an electromagnet are symmetrically located with respect to a median plane, the magnetic field at any point on the plane will be perpendicular to it. For an ion or electron moving in this plane the problem of describing its path reduces to a two-dimensional one.

For those cases where the magnetic field in the median plane can be expressed as a function only of one Cartesian coordinate, or as a function only of the radial distance from the axis of symmetry, for cases of circular symmetry, the equations describing the ion or electron paths admit of a simple treatment. Even if the dependence of the field upon such coordinates is known only experimentally, the complete solution may be determined by simple numerical integration to an accuracy equal to that with which the magnetic field is known. The general theory will be outlined and discussed below and certain cases analyzed in detail.

GENERAL THEORY

The Lorentz force equation for a charged particle in the presence of a magnetic field H and the absence of an electric field, is:

$$\mathbf{F}=\frac{e}{c}\mathbf{v}\times\mathbf{H}, \tag{1}$$

where e = charge of particle in e.s.u.; c = velocity of light; and $\mathbf{v}$ = velocity of particle in cm/sec.

* For an abstract of a preliminary report of this work see Phys. Rev. **65**, 352 (1944).

[1] While there is a vast literature on the general optics of charged particles moving in magnetic fields, applications of the type considered here do not appear to have been given specific treatment.

In addition to Eq. (1), we have the equation:

$$(\dot{x})^2+(\dot{y})^2+(\dot{z})^2=v^2=\text{const.},$$

since the magnetic field can do no net work on the charge. For the case of both Cartesian and cylindrical coordinates, we may, without loss of generality, consider H to be parallel to the z direction, so we then have:

$$\begin{aligned}(\dot{x})^2+(\dot{y})^2&=v^2,\\ (\dot{r})^2+(r\dot{\theta})^2&=v^2.\end{aligned}\tag{2}$$

Here v refers to the resultant velocity in a plane perpendicular to the z direction.

Written out in terms of Cartesian components, Eq. (1) becomes:

$$\begin{aligned}\ddot{x}&=-\frac{e}{mc}H\dot{y},\\ \ddot{y}&=\frac{e}{mc}H\dot{x},\end{aligned}\tag{3}$$

where H is the magnitude of the magnetic field, or:

$$\begin{aligned}\ddot{r}-r(\dot{\theta})^2&=-\frac{e}{mc}Hr\dot{\theta},\\ \frac{1}{r}\frac{d}{dt}(r^2\dot{\theta})&=\frac{e}{mc}H\dot{r},\end{aligned}\tag{4}$$

in cylindrical coordinates. Equations (3) and (4) cannot in general be solved explicitly if H is a function of both coordinates, as the equations will not be linear.

If, however, H is a function of only one coordinate, the equations are solvable in a simple manner, as follows:

Referring to Eq. (3), we may assume, without loss of generality, for this case that $H=H(x)$, and define a function $f=f(x)$ as:

$$f=\frac{e}{vmc}\int H(x)dx.\tag{5}$$

Integrating the second of Eqs. (3), we get:

$$\dot{y}=\frac{e}{mc}\int Hdx=vf.\tag{6}$$

However, from Eq. (2), we have:

$$\dot{x}=\pm(v^2-\dot{y}^2)^{\frac{1}{2}}=\pm v(1-f^2)^{\frac{1}{2}}.\tag{7}$$

Since $dy/dx=\dot{y}/\dot{x}$, we may combine Eqs. (6) and (7) to obtain:

$$\frac{dy}{dx}=\pm\frac{f}{(1-f^2)^{\frac{1}{2}}},\tag{8}$$

or:

$$y=\pm\int\frac{fdx}{(1-f^2)^{\frac{1}{2}}}.\tag{9}$$

We see thus that when H is a function of only one Cartesian coordinate, the equations of the trajectory are reduced to the simple differential equation (8), which permits immediate integration. When the magnetic field is a function only of the cylindrical coordinate r, the treatment is similar. For this case we define a function $g(r)$ by:

$$g(r)=\frac{e}{vmc}\frac{1}{r}\int rH(r)dr.\tag{10}$$

Integrating the second of Eqs. (4), we find

$$r\dot{\theta}=\frac{e}{rmc}\int rHdr=vg.\tag{11}$$

Using Eqs. (2) and (11), we have:

$$\dot{r}=\pm v(1-g^2)^{\frac{1}{2}},\tag{12}$$

and since $r\dot{\theta}/\dot{r}=r(d\theta/dr)$, we have from Eqs. (11) and (12):

$$\frac{d\theta}{dr}=\pm\frac{1}{r}\frac{g}{(1-g^2)^{\frac{1}{2}}},\tag{13}$$

or:

$$\theta=\pm\int\frac{gdr}{r(1-g^2)^{\frac{1}{2}}}.\tag{14}$$

We see, therefore, that the treatments for the Cartesian case and for the cylindrical case are similar, and involve essentially nothing more than two quadratures, either or both of which may be done numerically if not analytically.

Equations (5) and (10), which define f and g, will each contain a constant of integration. These constants may be used to specify the slope of the trajectory for any desired value of x or r by direct application of Eqs. (8) or (13). The

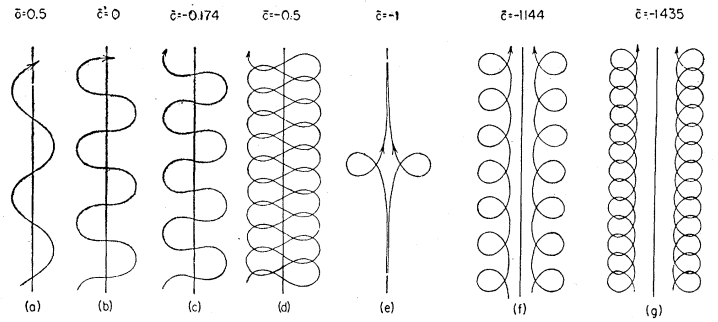

FIG. 1. Various types of orbits possible in a linearly varying magnetic field, determined by the parameter $\bar{c}$, defined by Eq. (17).

other initial condition, namely, the starting position in the x, y or θ, r plane is taken care of by the constant of integration in Eqs. (9) or (14).

The fact that the equations defining the trajectories involve the radical $(1-f^2)^{\frac{1}{2}}$ for the Cartesian case, and the radical $(1-g^2)^{\frac{1}{2}}$ for the cylindrical case, has a very simple and significant interpretation. Since these radicals must represent real magnitudes for any physically possible trajectory, we see immediately that the extension of the trajectory in the x or r coordinate will be given by $-1\leqslant f\leqslant 1$, or $-1\leqslant g\leqslant 1$, respectively.

If the equation

$$1-f^2=0 \tag{15}$$

has two real roots, the implication is that orbits will be bounded as regards extension in the x coordinate. This follows from the fact that dy/dx will be infinite for x equal to a real root of Eq. (15). If Eq. (15) has only one real root the orbit is one that comes in from and returns to plus or minus infinite values of x. For the case where Eq. (15) has two real roots the orbit will be either completely closed, or have an infinite extension in the y direction. The latter orbits will be of periodic behavior and will, in general, consist of an infinite number of loops of cycloidal appearance.

The same general considerations as just discussed for the case of Cartesian coordinates also hold for the cylindrical system and figures demonstrating them will follow in the detailed discussion of specific cases.

In the calculations for the paths in either coordinate system the quantity e/vmc enters as a fundamental constant of the motion. It is convenient to define this quantity as a, i.e.:

$$a=e/vmc.$$

In the discussion of many cases of physical interest it is more expedient to refer to the potential of a charged particle as a measure of its energy rather than to its velocity. We may, therefore, write a as

$$a=\frac{1}{c}\left(\frac{150e}{mV}\right)^{\frac{1}{2}},$$

where V is the potential of the particle in volts or its energy in electron volts.

LINEARLY VARYING MAGNETIC FIELD

The linear magnetic field may be defined by:

$$H=bx, \tag{16}$$

the origin being placed where the field is zero. From Eq. (5) it follows that:

$$f=a\int Hdx=\frac{abx^2}{2}+\bar{c}, \tag{17}$$

where $\bar{c}$ is the constant integration and $a=e/vmc$, as previously indicated.

Introducing the change of variables:

$$\bar{y}=\left(\frac{ab}{2}\right)^{\frac{1}{2}}y:\quad \bar{x}=\left(\frac{ab}{2}\right)^{\frac{1}{2}}x, \tag{18}$$

so that $\bar{y}$ and $\bar{x}$ are dimensionless, we find Eq. (8) takes the form:

$$\frac{d\bar{y}}{d\bar{x}}=\pm\frac{\bar{c}+\bar{x}^2}{[(1-\bar{c}-\bar{x}^2)(1+\bar{c}+\bar{x}^2)]^{\frac{1}{2}}}. \tag{19}$$

By inspection of the right side of this equation it is clear that if it is to represent a real trajectory $\bar{c}<1$. Moreover, the nature of the real trajectories will be determined by the magnitude of $\bar{c}$, as follows:

For $1>\bar{c}>-1$, the trajectories will all cross the y axis, with a slope $=\bar{c}/[1-\bar{c}^2]^{\frac{1}{2}}$. They will be symmetrical with respect to y, and the ion or electron will oscillate periodically between fixed values of x. If $1>\bar{c}>0$, the trajectory will simulate a sinusoidal oscillation with a monotonic increase or decrease in y, as illustrated in Fig. 1(a). When $\bar{c}=0$, the trajectories will have an inflection when crossing the y axis, as shown in Fig. 1(b), so that the change in y is still monotonic as the path is traversed. For $0>\bar{c}>-1$, the variation in y is no longer monotonic, and the trajectory tends to form loops as it oscillates between the fixed limits in x [cf. Fig. 1(c)]. At $\bar{c}=-0.46$, the loops of consecutive periods on either side of the x axis touch, and become interlaced [cf. Fig. 1(d)] as $\bar{c}$ is still further decreased. Complete overlapping of the loops, so as to form a single figure-eight trajectory, develops for $\bar{c}=-0.6522$. For the range $-0.6522>\bar{c}>-1$, they are again similar to a network of interlaced figure of eight oscillations, which spread out and ultimately degenerate into the single pair of split loops when $\bar{c}=-1$, as shown in Fig. 1(e).

In this whole range of $\bar{c}$ the maximum extension of the oscillations, which may be obtained from the roots of Eq. (15), continually increases as $\bar{c}$ decreases, according to the equation:

$$\bar{x}_{\max}=(1-\bar{c})^{\frac{1}{2}}. \tag{20}$$

Moreover, from the roots of Eq. (15) the width of the oscillations is given by:

$$\bar{x}_{\max}-\bar{x}_{\min}=(1-\bar{c})^{\frac{1}{2}}-(1+\bar{c})^{\frac{1}{2}}. \tag{21}$$

The detailed calculation of the trajectories may be readily made by introducing the substitution: $\bar{x}=(1-\bar{c})^{\frac{1}{2}}\cos\Phi$ and reducing the integral of Eq. (19) to standard elliptic integral form. It is thus found that:

$$\bar{y}=\frac{1}{\sqrt{2}}[2E(k)-K(k)-2E(\Phi,k)+F(\Phi,k)], \tag{22}$$

where $E(\Phi,k)$, $F(\Phi,k)$ are the incomplete elliptic integrals corresponding to E, K. It is to be noted that Eq. (21) applies directly only to the quarter-cycle of a single complete oscillation passing through the origin. Its continuation to both preceding and following elements of the trajectory is easily made by simple shifting of the initial point and appropriate changes in sign, as dictated by Eq. (19).

The wave-length, along y, of the oscillations is given by:

$$\lambda=2\sqrt{2}\,|2E(k)-K(k)|, \tag{23}$$

where K and E are the complete elliptic integrals of the first and second kind, the modulus $k=[(1-\bar{c})/2]^{\frac{1}{2}}$, and the absolute value is used to take care of the change in sign of the enclosed term at $\bar{c}=-0.6522$. λ is expressed in the same units as $\bar{y}$. It will be noted that $\lambda=4\bar{y}(\bar{x}_{\max})$.

In the limiting case $\bar{c}=-1$, integration of Eq. (19) readily gives:

$$\pm\bar{y}=\frac{1}{\sqrt{2}}\log\frac{\sqrt{2}+(2-\bar{x}^2)^{\frac{1}{2}}}{\bar{x}}-(2-\bar{x}^2)^{\frac{1}{2}},\quad \bar{x}>0, \tag{24}$$

from which were plotted the trajectories of Fig. 1(e).

The trajectories of greatest practical interest are those for $\bar{c}<-1$. The general features of these can also be deduced by direct inspection of Eq. (19). These no longer cross the $\bar{y}$ axis, but split up into two identically shaped individual trajectories, for each value of $\bar{c}$, placed symmetrically on the two sides of the $\bar{y}$ axis. Each of these is composed of a series of interlaced or separated loops extending from

$$|\bar{x}_{\max}|=(-1-\bar{c})^{\frac{1}{2}},\quad \text{to}\quad |\bar{x}_{\min}|=(1-\bar{c})^{\frac{1}{2}}, \tag{25}$$

and hence recede from the $\bar{y}$ axis as $\bar{c}$ is decreased. The overlapping of the loops increases as $\bar{c}$ decreases [cf. Figs. 1(f) and 1(g)]. The wave-length is given by:

$$\lambda=2(1-\bar{c})^{\frac{1}{2}}\left[\left(1-\frac{k^2}{2}\right)K-E\right] \tag{26}$$

where now the modulus $k=[2/(1-\bar{c})]^{\frac{1}{2}}$. A plot of λ and $(\bar{x}_{\max}-\bar{x}_{\min})$ *vs.* $\bar{x}_{\max}$ is given in Fig. 2. It will be seen that both λ and the lateral range of the oscillations decrease as $\bar{x}_{\max}$ increases—i.e., as the trajectories are confined to regions of greater magnetic field. This is, of course, to be expected from elementary considerations.

For calculating the exact shape of the trajectories for this range of $\bar{c}$, the integral of Eq. (19) may again be transformed into standard elliptic integrals, by setting $\bar{x}^2=\cos 2\Phi-\bar{c}$ with the result that:

$$\bar{y}=(1-\bar{c})^{\frac{1}{2}}[E(\Phi, k)-(1-\tfrac{1}{2}k^2)F(\Phi, k)]. \quad (27)$$

As remarked above, orbits of the type illustrated in Figs. 1(f) and 1(g) are of greatest interest. This is because of the practical difficulty of obtaining a field variation in which H is an odd linear function of x. Also, for any restricted region of an actual non-uniform field H may be considered linear with distance to a first approximation. The orbits calculated from Eq. (19) will therefore represent the actual paths of the ions or electrons to at least a first approximation. Application of such orbits as in Figs. 1(g) and 1(f) to magnetic focusing instruments will be discussed below.

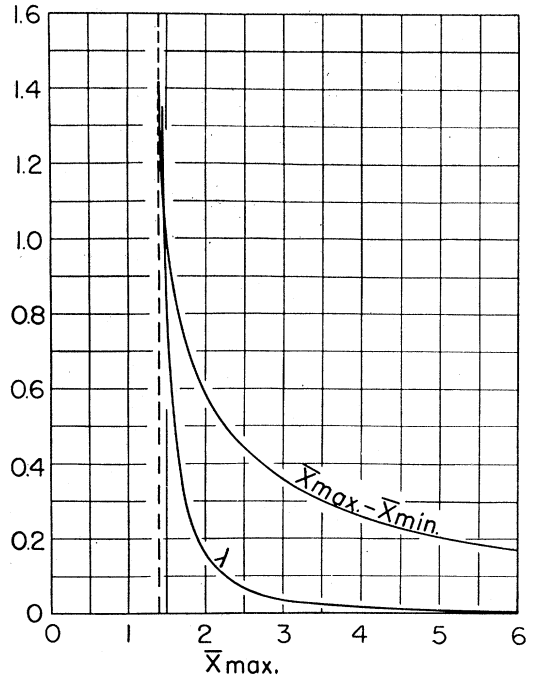

FIG. 2. The variation of the dimensionless wave-length λ and lateral range $\bar{x}_{\max}-\bar{x}_{\min}$, of periodic orbits in a linearly varying magnetic field, with the maximal extension $\bar{x}_{\max}$.

EXPONENTIALLY VARYING FIELD

For the case of an exponentially varying field in Cartesian coordinates we may write H as:

$$H=H_0e^{bx},$$

where H_0 is the magnitude of the field strength at the value of x chosen as the origin of the coordinate system, and b is the constant determining the rate of change of H with x.

The function f then becomes:

$$f=\frac{aH_0}{b}e^{bx}+\bar{c}, \quad (28)$$

where $\bar{c}$ is a constant of integration which may be adjusted to give the orbit the desired slope at any value of x. For this case Eq. (8) becomes:

$$\frac{dy}{dx}=\pm\frac{\frac{aH_0}{b}e^{bx}+\bar{c}}{\left\{1-\left(\frac{aH_0}{b}e^{bx}+\bar{c}\right)^2\right\}^{\frac{1}{2}}}. \quad (29)$$

By making the transformation:

$$v=\frac{aH_0}{b}e^{bx},$$

Eq. (29) may be readily integrated to give the general solution:

$$y=\pm\frac{1}{b}\left\{\sin^{-1}(v+\bar{c})-\frac{\bar{c}}{(1-\bar{c}^2)^{\frac{1}{2}}}\right.$$
$$\left.\times\log\left[\frac{\{1-(v+\bar{c})^2\}^{\frac{1}{2}}+(1-\bar{c}^2)^{\frac{1}{2}}}{v}-\frac{\bar{c}}{(1-\bar{c}^2)^{\frac{1}{2}}}\right]\right\}, \quad (30)$$

when $|\bar{c}|<1$, and

$$y=\pm\frac{1}{b}\left\{\sin^{-1}(v+\bar{c})\right.$$
$$\left.+\frac{\bar{c}}{(\bar{c}^2-1)^{\frac{1}{2}}}\sin^{-1}\left[\frac{1-\bar{c}^2-\bar{c}v}{v}\right]\right\}, \quad (31)$$

when $\bar{c}<-1$.

For the special case, $\bar{c}=-1$,

$$y=\pm\frac{1}{b}\left\{2\sin^{-1}\left(\frac{v}{2}\right)^{\frac{1}{2}}+\frac{(2v-v^2)^{\frac{1}{2}}}{v}\right\}.$$

Orbits defined by Eq. (30) are illustrated by (a), (b), and (c) in Fig. 3. In each case the particle enters the magnetic field from $x=-\infty$, or, physically speaking, from a region of very weak H. As must obviously be the case, each orbit is symmetrical about the x axis. Each path

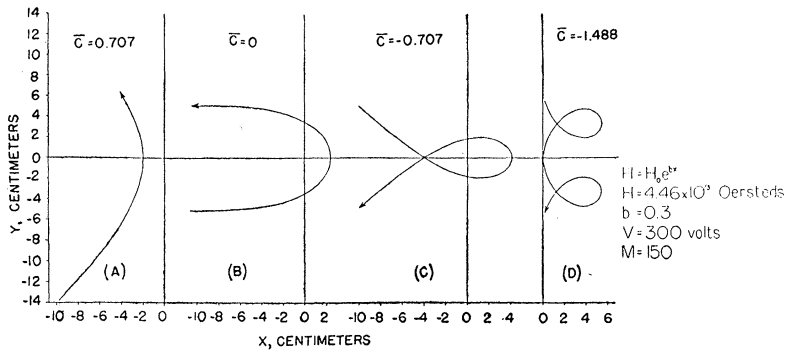

FIG. 3. Various types of orbits possible in an exponential magnetic field, determined by the parameter $\bar{c}$, defined by Eq. (28). All orbits are for singly-charged particles of 300-ev energy and 150 atomic mass units. *Note:* The second line of the explanation at the right of the cut should read $H_0=4.46\times10^3$ oersteds.

is shown in the neighborhood of $H=H_0$, which establishes the origin of the x coordinate. Orbits (a), (b), and (c) represent a particle of 150 atomic mass units and 300 electron volts energy coming from $x=-\infty$ with initial slope of 1, 0, and -1, respectively. Orbit (d) is for a particle of the same mass and energy but so projected in the x, y plane that the path has infinite slope at $x=0$.

Orbits of the type illustrated by (b) are of particular interest, as the total extension in the y direction depends only on the exponential coefficient b, and is independent of the values of the mass and velocity of the ion or electron. This fact is immediately seen upon setting $\bar{c}=0$ in Eq. (30), which physically corresponds to the particles approaching regions of stronger magnetic field with an original direction parallel to the x direction. This situation affords an opportunity for perfect focusing, further discussion of which will be given later.

If the ion or electron is introduced into the magnetic field in such a manner that its subsequent orbit is bounded in the x direction, it will be of the type illustrated by (d), Fig. 3. This type of orbit is also of interest as regards application to focusing problems, and will be discussed in more detail below. For this type trajectory the total width in the x dimension is readily calculated from the separation of the roots of Eq. (15).

The behavior of orbits of type (d) as regards their total width in the x direction and their wave-length λ can be discussed in a manner similar to that used for the linearly varying field. For a particular value of $\bar{c}$ we have:

$$x_{\max}=\frac{1}{b}\log\frac{b}{aH_0}(1-\bar{c}),$$
$$x_{\min}=\frac{1}{b}\log\frac{b}{aH_0}(-1-\bar{c}). \tag{32}$$

As $\bar{c}<-1$ for all such orbits the arguments of the logarithms will be positive. We may express $x_{\max}-x_{\min}$ as a function of $x_{\max}$ by eliminating $\bar{c}$ in Eqs. (32) to give:

$$x_{\max}-x_{\min}=x_{\max}-\frac{1}{b}\log\left(e^{bx_{\max}}-\frac{2b}{aH_0}\right),$$

which behaves qualitatively like the similar quantity for the linear case which is plotted in Fig. 2.

From the nature of Eq. (31) it is seen that the orbits are periodic with a wave-length of λ given by:

$$\lambda=\frac{2\pi}{b}\left(1+\frac{\bar{c}}{(\bar{c}^2-1)^{\frac{1}{2}}}\right),$$

or

$$\lambda=\frac{2\pi}{b}\left[1+\frac{1-\frac{aH_0}{b}e^{bx_{\max}}}{\left[\left(1-\frac{aH_0}{b}e^{bx_{\max}}\right)^2-1\right]^{\frac{1}{2}}}\right]. \tag{33}$$

RADIAL FIELDS

Although Eqs. (10) and (14) make it possible to determine the path of a charged particle in

any field of circular symmetry, the functional variation of H we shall discuss here is given by:

$$H=\frac{H_0}{r^{n+1}},$$

where $n>-1$, and H_0 is a constant. It will, of course, be physically impossible for H to obey this relation for values of r including the origin. However, it will suffice if the relation is obeyed within certain limits of r, or for values of r above a definite radius.

For this case (and $n\neq 1$) $g(r)$ becomes:

$$g=\frac{aH_0}{(1-n)r^n}+\frac{\bar{c}}{r}, \tag{34}$$

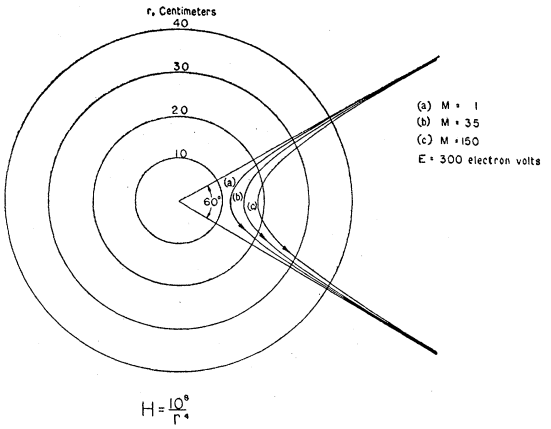

FIG. 4. Non-periodic orbits with common asymptotes in a radially varying magnetic field, with $n=3$, for singly-charged particles of 300 ev and various atomic masses M.

and we have:

$$\theta=\pm\int\left(\frac{aH_0}{(1-n)r^{n+1}}+\frac{\bar{c}}{r^2}\right)\Big/\left[\left(1-\left\{\frac{aH_0}{(1-n)r^n}+\frac{\bar{c}}{r}\right\}^2\right)\right]^{\frac{1}{2}}dr. \tag{35}$$

Equation (35) is in general more amenable to numerical than analytical treatment.

One case of important physical interest does, however, admit of simple analytical treatment. This is that of charged particles approaching regions of strong H from regions of weak H, and with an initial direction along a radius vector and toward the axis of symmetry.

Before discussing the solution for this particular case it will be of interest to examine the general features of the orbits defined by Eq. (35). It will be noted first, from Eq. (34), that if $n>0$ $(\neq 1)$, $g(r)\to 0$ as $r\to\infty$. Hence by Eq. (13), $r(d\theta/dr)\to 0$ as $r\to\infty$. This means that for $n>0$ $(\neq 1)$ all orbits entering the field from infinity must be asymptotically parallel to a radius vector. As all radii vectors are equivalent, these orbits may thus be considered as necessarily entering the field parallel to the polar axis $(\theta=0)$. If, in particular, these orbits asymptotically degenerate into linear paths at a normal distance h from the polar axis, i.e., so that

$$r\sin\theta=h,$$

then it follows that in the limit as $r\to\infty$,

$$r\frac{d\theta}{dr}\longrightarrow-\frac{h}{r\cos\theta}\sim-\frac{h}{r}\sim g.$$

By Eq. (34), such an asymptotic behavior can be satisfied only if $n>1$ and $\bar{c}=-h$. Accordingly, in inverse power radial fields for which $n>1$, $-\bar{c}$ is simply the normal distance from the polar axis with which the particle enters the field. The restriction $n>1$ evidently means that if $n<1$ there can be no orbits which enter the field along linear paths parallel to a radius vector. If $0<n<1$ the value of $\bar{c}$ can be determined by fixing $r(d\theta/dr)$ at a given radius, computing g from Eq. (13), and then $\bar{c}$ by Eq. (34).

If $n=0$, the orbits entering or leaving the field at $r=\infty$ will asymptotically cut the radii vectors at an angle $\sin^{-1}aH_0$. For this case the integral for $\theta(r)$ can be readily evaluated to give expressions similar to Eqs. (30) and (31). If $-1<n<0$ the orbits will be restricted to finite regions of the (r,θ) plane, and be bounded by a maximum value of r.

Returning to the special case $n>1$, and also assuming that the particle actually enters the field along the polar axis $(\bar{c}=0)$, we may readily integrate Eq. (35) and obtain:

$$\theta=\pm\frac{1}{n}\sin^{-1}\frac{aH_0}{(1-n)r^n}. \tag{36}$$

Orbits of this type for $n=3$ are plotted in Fig. 4. It is interesting to note that these orbits

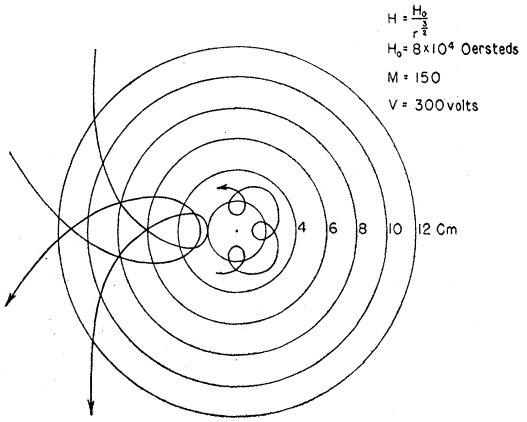

FIG. 5. Typical orbits in a radially varying magnetic field, with $n=\frac{1}{2}$, which are convex to the origin at $r=r_{\min}$.

have an angular spread independent of mass and energy, quite analogous to those for the exponentially varying field in Cartesian coordinates, shown in Fig. 3(b). These trajectories will be discussed in more detail later.

Other types of orbits obtainable in radial fields are illustrated in Figs. 5 and 6. In Fig. 5 the particles are so projected, in a field with $n=\frac{1}{2}$, that the paths are convex with respect to the origin at the points of closest approach. These were determined by numerical integration of Eq. (35), after choosing the point of minimum approach and determining the corresponding value of $\bar{c}$. In a similar manner were computed the orbits shown in Fig. 6, which are concave to the origin at the points of closest approach. In Fig. 5 may be seen a periodic or cyclic type of orbit of the same general properties as possessed by the periodic orbits in the Cartesian coordinate cases.

For periodic orbits, the equation

$$1-g^2=0,$$

which is analogous to Eq. (15) for the Cartesian case, must have two real and unequal roots. For a given value of n and $\bar{c}$ it is possible to determine whether the resulting orbit will be periodic or not by determining whether g will pass through both the values -1 and $+1$ as r is increased.

APPLICATIONS

In addition to illustrating the application of the general method of calculation given above to specific cases, the orbits previously discussed have certain characteristics of promise for instruments such as mass spectrometers, mass spectrographs, beta-ray spectrometers, etc. For example, Fig. 7 illustrates the orbits of ions of masses 1, 35, and 150, expressed in atomic mass units, and all having a kinetic energy of 300 electron volts. The type of equation which describes these orbits, as well as that of Fig. 3(b), is obtained by setting $\bar{c}=0$ in Eq. (30), giving

$$y=\pm\frac{1}{b}\sin^{-1}\left(\frac{aH_0}{b}e^{bx}\right). \tag{37}$$

From these figures and Eq. (37) it is seen that all such ions which initially approach an exponentially varying field in the direction of increasing H will turn and recede in an opposite direction. Also, the ions will recede asymptotically to a line displaced from their original line of approach by an amount independent of the momentum of the particle and depending only upon the exponential coefficient b.

With this arrangement all ions beginning at a point where the field is negligibly weak, and with a direction toward regions of increasing H, will return to a single point where the magnetic field is also negligibly weak.

A schematic diagram of an instrument which might be designed to utilize this type of orbit may be seen in Fig. 8. The design shown here is for a mass spectrometer, but with obvious changes it could be used as a beta-ray spec-

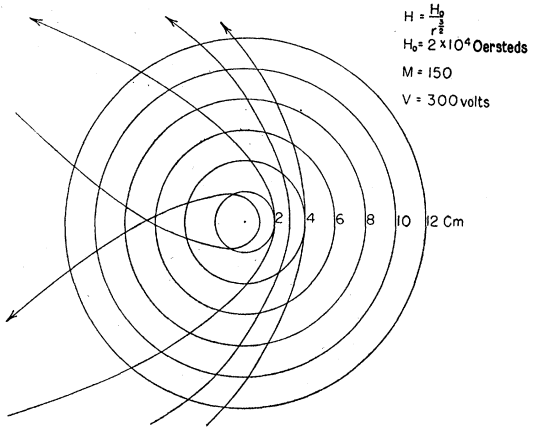

FIG. 6. Typical orbits in a radially varying magnetic field, with $n=\frac{1}{2}$, which are concave to the origin at $r=r_{\min}$.

trometer, or for special studies such as electron or ion scattering, etc. By adjusting an aperture or slit, located as shown in Fig. 8, the instrument may be made to focus either only particles of a narrow momentum range, such as ions of a definite mass, or particles of a wide momentum or energy range. An idea of the amount of dispersion taking place at the region of the slit may be obtained by inspection of Fig. 7, which represents paths of physical interest. The separation in the turning points of any two ion beams of momentum parameters a_1 and a_2 may be readily calculated from Eq. (37), which gives

$$x_1-x_2=\frac{1}{b}\log\frac{a_2}{a_1}=\frac{1}{b}\log\frac{(mv)_1}{(mv)_2}.$$

For an instrument such as this, it would be necessary for the magnetic field to vary in an exponential manner only over a region large enough to encompass the dimensions of the instrument.

In designing pole pieces of an electromagnet so as to obtain an exponentially varying field, the first requirement is to have the dimension in the direction perpendicular to the x, y plane long compared to the size of the instrument desired, so as to allow the field to be accurately two dimensional. Next it would be necessary that the design be such that the three equations:

$$\frac{\partial^2 M}{\partial x^2}+\frac{\partial^2 M}{\partial z^2}=0, \tag{38}$$

$$\left.\begin{aligned}\frac{\partial M}{\partial x}&=0\\ \frac{\partial M}{\partial z}&=H_0e^{bx}\end{aligned}\right\}\text{at } z=0, \tag{39}$$

be satisfied, where M represents magnetostatic potential.

A solution of Eq. (38), which also satisfies Eqs. (39), is:

$$M=\frac{H_0e^{bx}}{b}\sin bz.$$

If the magnetostatic potentials of the opposing pole faces are $+M_0$ and $-M_0$, respectively, we have the equation:

$$z=\pm\frac{1}{b}\sin^{-1}\left(\frac{bM_0e^{-bx}}{H_0}\right), \tag{40}$$

to define the contours of the pole faces.

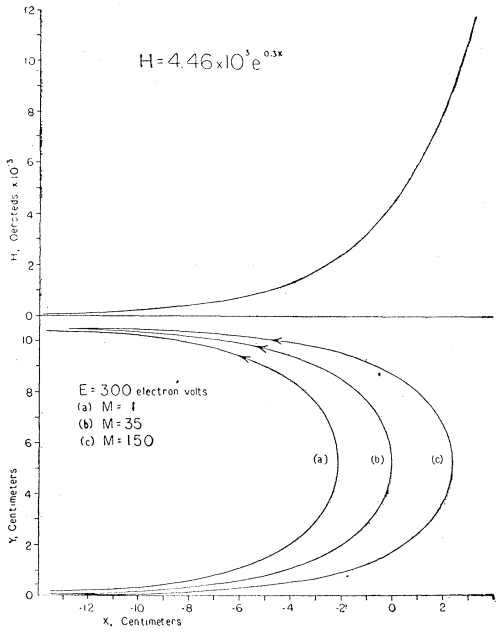

FIG. 7. Typical orbits with common asymptotes in an exponentially varying magnetic field.

In Fig. 4 are seen orbits which, for the case of radially symmetric fields, are analogous to the orbits just discussed. They are defined by Eq. (36). It is obvious that since these orbits are analogous to those of Figs. 7 and 5, the same focusing properties could be applied in corresponding instruments. As for the Cartesian exponential field, the optics of the radial field system is such that ions originating at a point where the field is negligibly weak, i.e., at "infinity," and with an initial velocity toward the center of symmetry of the field, will be all focused, regardless of their individual momenta, at another single point. This point will be on a radius vector which is rotated from the line of approach radius vector by an angle which depends only upon the exponent in the equation defining the variation of H with r. It must also be remembered that orbits with this property are possible only for $n>1$ in Eq. (34).

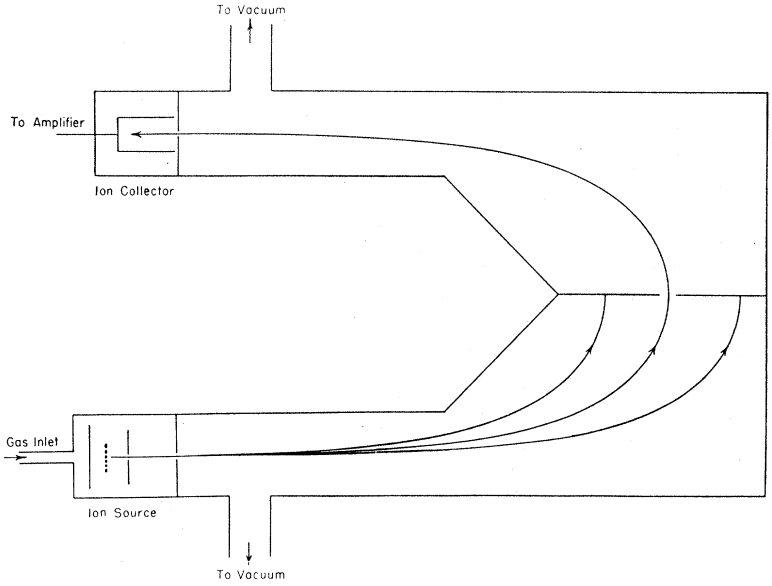

FIG. 8. Schematic diagram of a magnetic analyzer utilizing an exponentially varying magnetic field.

A schematic diagram of an instrument designed to employ this type of orbit is shown in Fig. 9. An idea of the dispersion obtainable may be seen from Fig. 4, and may be expressed analytically as:

$$\frac{\Delta r}{r}=\frac{1}{n}\frac{\Delta a}{a}=\frac{1}{n}\frac{\Delta(mv)}{mv},$$

where r and $r+\Delta r$ are the turning radii for particles of parameters a and $a+\Delta a$. Fields which decrease with radial distance with the same functional form have been successfully used in the betatron.[2]

To obtain the field variation just discussed the circularly symmetric pole faces must be so shaped that the following equations are satisfied:

$$\frac{\partial}{\partial r}\left(r^2\frac{\partial M}{\partial r}\right)+\frac{1}{\sin\Phi}\frac{\partial}{\partial\Phi}\left(\sin\Phi\frac{\partial M}{\partial\Phi}\right)=0, \quad (41)$$

$$\left.\begin{aligned}\frac{\partial M}{\partial r}&=0,\\ \frac{1}{r}\left(\frac{\partial M}{\partial\Phi}\right)&=\frac{H_0}{r^{n+1}},\end{aligned}\right\}\Phi=\pi/2, \quad (42)$$

[2] D. W. Kerst, Phys. Rev. **60**, 47 (1941).

where M is the magnetostatic potential, and Φ is the latitude angle.

Setting $\mu=\cos\Phi$, and $M=(H_0/r^n)F(\mu)$, we find $F(\mu)$ must satisfy the Legendre equation:

$$(\mu^2-1)\frac{d^2F}{d\mu^2}+2\mu\frac{dF}{d\mu}-n(n-1)F=0.$$

To fix the specific solutions for $F(\mu)$ applying to the present problem, the equivalents of Eq. (42), namely: $F(0)=0$; $F'(0)=-1$, are to be imposed on the functions $F(\mu)$.

If we let the opposite pole faces have magnetostatic potential $+M_0$ and $-M_0$, the contours will be given by:

$$r=\left\{\frac{H_0F(\theta)}{\pm M_0}\right\}^{1/n}, \quad (43)$$

the sign of $F(\theta)$ automatically changing in passing from one pole face to the other, so as to ensure a real value for r.

As the region over which it is desired that H have the specified functional form will not extend to the origin, the pole faces in this region need not follow the shape required by Eq. (43). This physical observation also obviates the apparent difficulty arising from the singularities at $\mu=\pm1$ in the functions $F(\mu)$ when n is not an integer.

The periodic or cyclic orbits of the type in Figs. 1(f) and (g), and Fig. 3(d), also have properties of promise for focusing applications. One of the most important of these properties is illustrated in Fig. 2. This shows how the wave-length λ, or spatial periodicity of the orbit, decreases with increasing x_{max}. This curve was drawn for H varying linearly with x, but its character will be essentially the same for other functional variations wherein H increases monotonically with increasing x.

An application of such orbits may be made to the design of a mass spectrometer or similar instrument, as indicated schematically in Fig. 10. In such an instrument the ions are so accelerated by a suitable source that they are projected into the magnetic field with the x_{max} for each orbit lying within the exit slits.

In Fig. 11 may be seen a schematic diagram of the state of affairs at the exit slits S_1 and S_2 of such an ion source. We shall assume that the potential distribution in the source is such that all ions acquire essentially the same potential, and that the last two slits, i.e., S_1 and S_2 in Fig. 11, are at the same potential and are operative only in defining the emergent beam. Moreover, these slits will be assumed to be geometrically similar and located identically as regards the x coordinate.

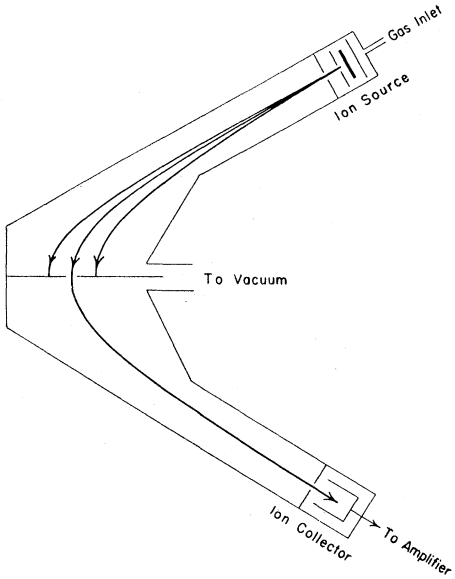

FIG. 9. Schematic diagram of a magnetic analyzer utilizing a radially varying magnetic field.

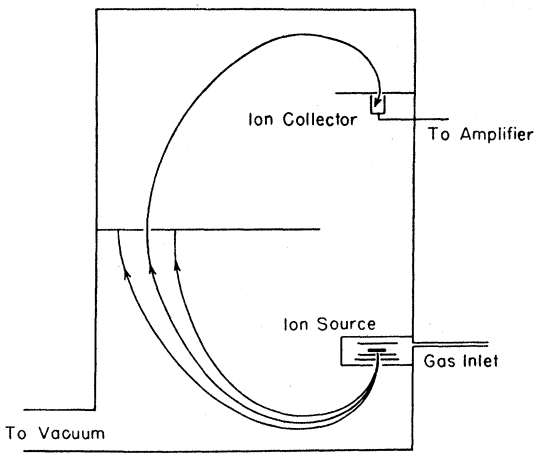

FIG. 10. Schematic diagram of a magnetic analyzer utilizing periodic orbits in an exponentially varying magnetic field.

With such an arrangement all ions leaving the exit slits will follow orbits having approximately the same radius of curvature at the slits, differing only in the angle of emergence.

In Fig. 11, (c) represents the orbit with the smallest value of x_{max} that can emerge from the slits, (d) that with the largest value of x_{max}, while (a) and (b) represent the paths of greatest divergence in angle of emergence. As S_1 and S_2 cover the same range along the x direction, the x_{max} will be the same for orbits (a) and (b).

Consider now the orbits (a), (b), (c), and (d) when the particles have advanced by exactly one wave-length in their periodic paths. Since (a) and (b) have the same x_{max}, they will have the same λ. Therefore a slit S_1' of the same width as S_1 and located at the same values of x, but displaced along y by a distance λ, will collect both (a) and (b). That is, (a) and (b) will pass through S_1' with exactly the same geometry as they passed through S_1. As orbit (c) has a smaller value of x_{max}, it will be displaced slightly upward, relative to (a) and (b). Conversely, as orbit (d) has a larger value of x_{max}, its λ will be smaller than that of (a) and (b). Hence as it passes through S_1' it will be displaced slightly downward relative to (a) and (b).

This shifting of the orbits (c) and (d) relative to (a) and (b) means that the latter will limit the lateral spread in the ion beam when entering S_1' just as they defined the angular spread in

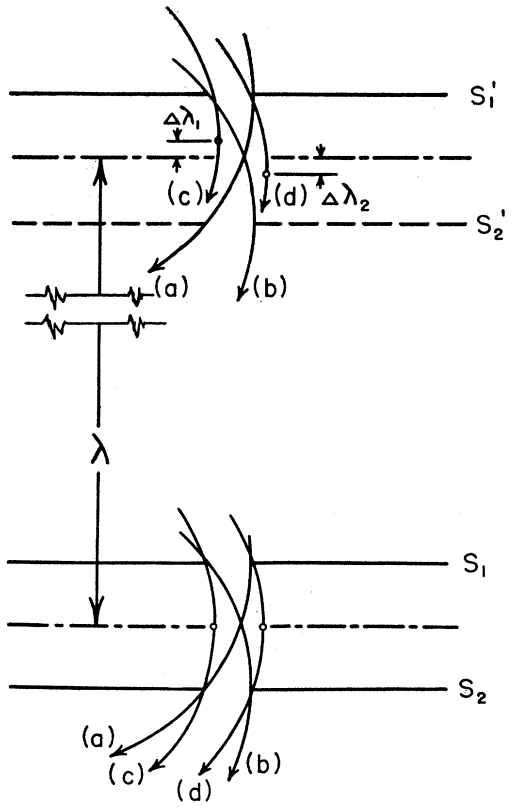

FIG. 11. Schematic diagram of the geometry of the orbits at the source and collector slits of an instrument of the type shown in Fig. 10.

the beam emerging from the source slits S_1 and S_2. In the design of such an instrument, as schematically shown in Fig. 10, the final two exit slits will correspond to S_1 and S_2, and the collector slit should be of the same dimensions as S_1 and located at the same distance along the x axis. The separation along the y axis between S_1 and S_1' will then define the wave-length λ for which the above-described focusing process applies. Any ion may be made to follow an orbit of any chosen λ by properly fixing the accelerating voltage in the ion source. It is to be noted that for the collector the one slit S_1' is sufficient. S_2' is shown in Fig. 11 only to indicate the geometry of the orbits at this point. If the instrument is to be used so that only ions of one mass or of small range of momentum are to pass the collector, an aperture or slit may be introduced, as shown in Fig. 10.

The calculation of the dispersion at the region of the selector slit or aperture is easily made by application of Eq. (29). For this purpose it is convenient to choose the origin at the exit slits of the ion source. Then, since $dy/dx=\infty$ at the ion source ($x=0$), $\bar{c}$ must have the value

$$\bar{c}=1-\frac{aH_0}{b}.$$

At the turning point of the orbit, i.e., at the plane of the selecting slits, $dy/dx=\infty$ again, so that:

$$\bar{c}+\frac{aH_0}{b}e^{bx}=-1,$$

giving for the location of the turning point:

$$x=\frac{1}{b}\log\left\{1-\frac{2b}{aH}\right\}.$$

For two ion beams of momentum parameters a_1 and a_2 the turning points will then be separated by a distance:

$$(x_1-x_2)=\frac{1}{b}\log\left\{\frac{1-\dfrac{2b}{a_1H}}{1-\dfrac{2b}{a_2H}}\right\}.$$

A similar type of instrument could be designed using the periodic orbits in a radial field, such as shown in Fig. 5. Similar considerations with respect to focusing and the use of selector slits will be applicable to such instruments. Finally, it should be noted that the above discussion has referred to particles moving in the median plane between the pole pieces generating the magnetic field. Hence in practical designs account will have to be taken of the perturbations in the orbits of particles off the median plane owing to the curvature of the magnetic flux lines.

The authors are indebted to Mr. N. F. Kerr for assistance in preparing the drawings and making the calculations, and to Dr. P. D. Foote, Executive Vice President of The Gulf Research and Development Company, for permission to publish this paper.